Study of entropy production due to electroweak phase transition in Z_2 symmetric extension of the Standard Model

Arnab Chaudhuri[1,2,*] and Jaydeb Das[3,†]

[1]*Institute of Physics, Bhubaneswar, Bhubaneswar 751005, India*
[2]*Homi Bhabha National Institute, Mumbai 400085, India*
[3]*Department of Physics and Astrophysics, University of Delhi, Delhi 110007, India*

(Received 8 August 2022; accepted 24 October 2022; published 15 November 2022)

In this work, we consider the simple Z_2 symmetric extension to the Standard Model (SM) and proceed to study the nature of electroweak phase transition (EWPT) in the early Universe. We show that the nature of the phase transition changes from a smooth crossover in the SM to a strong first order with this addition of the real scalar. Furthermore, we show that the entropy release in this scenario is higher than that of the SM. This can lead to a strong dilution of the energy density of gravitational waves, as we show in the latter part of the paper.

DOI: 10.1103/PhysRevD.106.095016

I. INTRODUCTION

The Standard Model (SM) of particle physics is successful in describing three of the four known fundamental forces (electromagnetic, weak, and strong) in the Universe and classifying all known elementary particles. Although the SM is one of the most popular theories at the current moment, it leaves some phenomena unexplained. It falls short of being a complete theory of fundamental interactions. For example, it does not fully explain baryon asymmetry, incorporate the full theory of gravitation [1] as described by general relativity, or account for the Universe's accelerating expansion as possibly described by dark energy, and further does not contain any viable candidate for dark matter.

The predominance of matter over antimatter—i.e., the mechanism of baryogenesis—follows Sakharov's principle [2], and is due to (i) the nonconservation of baryon numbers, (ii) the breaking of C and CP invariance, and (iii) deviation from thermal equilibrium. For a successful explanation of the baryon asymmetry [3,4] in the Universe through baryogenesis, a strong first-order electroweak phase transition (EWPT) in the early Universe is necessary. Cosmic EWPT happened when the hot Universe cooled down enough in the primeval time so that the potential of the Higgs field settled at a nonzero minimum, and in consequence, the symmetry of the theory $SU(3)_C \times SU(2)_L \times U(1)_Y$ broke to $U(1)_{\mathrm{em}}$. At the time of first-order EWPT, bubbles of the broken phase originate, and baryon-antibaryon asymmetry generates outside the wall of the bubbles of the broken phase. However, after the discovery of the SM Higgs boson [5], it became more obvious that EWPT within the framework of the SM is a smooth crossover phase transition—see Refs. [6,7]. Hence, for a successful electroweak baryogenesis (EWBG), the theory of EWPT should be of first order, and hence a theory beyond the SM is necessary. Strong first-order phase transition in the Z_2 and Z_3 extensions of the SM are studied in Refs. [8–11].

On the other hand, ∼26.5% of the total energy density of the Universe is contributed by dark matter (DM), whose origin is still a mystery. Even though primordial black holes (PBHs) and MACHOs are considered to be viable baryonic DM candidates, it is now clear that they are unable to contribute sufficiently to completely account for the DM energy density of the Universe. There are theories about multicharged extensions of the Standard Model like dark atoms, which may be viable dark matter candidates [12], but there is presently no experimental evidence of such. Not only can the SM not explain the phenomenon of successful baryogenesis, but there are no irrefutable theories in the SM about nonbaryonic DM particles which can successfully explain all the observations.

Due to these shortcomings of the SM, the search for beyond Standard Model (BSM) physics has become a hot topic among physicists nowadays. For them, the recent result from Fermilab about $g_\mu - 2$ for muons may be a ray of hope. g_μ is the gyromagnetic ratio of the muon, which is defined as the ratio of the magnetic moment to the angular moment of the muon, and whose value is 2 from tree-level

*arnabchaudhuri.7@gmail.com
†Corresponding author.
jaydebphysics@gmail.com

calculation. If we define $a_\mu = (g_\mu - 2)/2$, then higher-order loop corrections from SM give $a_\mu = 116,591,810(43) \times 10^{-11}$, where the value measured from Fermilab is $16,592,061(41) \times 10^{-11}$, which differs from the SM at the 3.3σ level [13]. This contradiction is actually buttressed by the previously claimed result from the E821 experiment at Brookhaven National Lab (BNL). There are numerous explanations for this anomalous result, including the existence of BSM physics.

The early Universe is often associated with thermal equilibrium and negligible chemical potential. During the course of the Universe's expansion, the entropy density per comoving volume was conserved, and the conservation law follows

$$s = \frac{\rho + \mathcal{P}}{T} a^3 = \text{const.}, \tag{1}$$

where ρ and $\mathcal{P}$ are the energy and the pressure density of the plasma, respectively; T is the temperature of the plasma; and a is the cosmological scale factor. In thermal equilibrium, the distribution function of any particle species is determined by the chemical potential μ_i of each particle type and the temperature of the plasma. But in the case of thermal inequilibrium, the entropy conservation law breaks down. Several instances of entropy nonconservation include QCD phase transition at $T \sim 150$ MeV—for review, see Ref. [14]. If PBHs of sufficiently small mass dominated the Universe at a certain point during the course of its evolution, the evaporation of such PBHs could lead to the influx of sufficient entropy into the plasma. For details and review, see Refs. [15,16].

Another source of entropy production, which is the primary focus of this paper, is due to EWPT. Possibly the largest entropy release in the Standard Model took place in the process of the EWPT from the symmetric to the asymmetric electroweak phase in the course of the cosmological cooling down. In principle, the transition could be either first order or second order, or even a very smooth crossover. Within the framework of the SM with a single Higgs, the phase transition is crossover in nature. But in extended theories of the SM, it can be of first order [17–22].

In this work, we consider a Z_2 symmetric singlet scalar extension to the SM. We show that this simple inclusion changes the nature of the EWPT from a smooth crossover to a first-order phase transition. We further proceed to calculate the entropy release during the first-order phase transition and show that it is considerably higher than the SM scenario, even with a single singlet scalar extension. The paper is arranged as follows: In Sec. II, the details about the potential along with the correction terms are shown. The next section gives details about the nature of the phase transition and the calculation of entropy production. Section V shows the connection of the entropy release to observations—namely, the dilution of the energy density of gravitational waves. This is followed by a generic conclusion and discussion.

II. TREE-LEVEL POTENTIAL

In our framework, we extend the SM by a real scalar which transforms as a singlet under the SM gauge group. We call this extra singlet the bosonic degree of freedom S. In addition to the SM gauge symmetry, we impose an extra Z_2 symmetry (i.e., $S \to -S$) on the scalar potential, so that we can exclude all odd-powered terms of S in the Lagrangian. So, the tree-level potential consists of the pure Higgs potential of the SM along with the quadratic and quartic terms of S and a portal term, which is essentially an interaction term between the singlet scalar and the SM Higgs field. So, the renormalizable tree-level potential with a real singlet scalar extension to the Standard Model consists of the scalar field S and the Higgs doublet ϕ, given by

$$V(\phi, S) = -\mu_h^2 \phi^\dagger \phi + \lambda_h (\phi^\dagger \phi)^2 - \frac{1}{2}\mu_S^2 S^2 + \frac{1}{4}\lambda_S S^4 + \frac{1}{2}\lambda_m S^2 (\phi^\dagger \phi). \tag{2}$$

In the above Eq. (2), μ_h^2 and μ_S^2 are the bare parameters with mass dimension 2, while λ_h and λ_S are the dimensionless quartic coupling constants for the Higgs doublet ϕ and singlet scalar field S, respectively. There is another dimensionless coupling constant λ_m, called the Higgs portal coupling, related to the SM Higgs and the singlet scalar interaction term in the tree-level potential. Because of the extra Z_2 symmetry, we do not include the terms which are linear and cubic in S in the potential.

The SM Higgs doublet ϕ can be written as

$$\phi = \frac{1}{\sqrt{2}} \begin{pmatrix} \chi_1 + i\chi_2 \\ h + i\chi_3 \end{pmatrix}, \tag{3}$$

where χ_1, χ_2, and χ_3 are three Goldstone bosons, and h is the Higgs boson. The tree-level potential in terms of the classical background fields h and S reads as

$$V_0(h, S) = -\frac{1}{2}\mu_h^2 h^2 + \frac{1}{4}\lambda_h h^4 - \frac{1}{2}\mu_S^2 S^2 + \frac{1}{4}\lambda_S S^4 + \frac{1}{4}\lambda_m S^2 h^2. \tag{4}$$

It needs to be mentioned here that the classical background fields h and S in Eq. (4) are not the same as those of Eqs. (2) and (3). After expanding the potential around the classical background fields, we obtain the above Eq. (4).

We are interested in studying the strong first-order electroweak phase transition in that scenario where at higher temperatures electroweak symmetry is present, but discrete Z_2 symmetry is spontaneously broken by

the vacuum expectation value (VEV) of the singlet scalar. When temperature gradually decreases, the SM Higgs field gets a VEV, but the singlet scalar has no VEV. In other words, at lower temperatures, Z_2 symmetry is present, but SM gauge symmetry is spontaneously broken by the VEV of the Higgs field. Therefore, at zero temperature, the SM Higgs has a VEV of $v_{\rm EW} = 246$ GeV, but the singlet scalar has no VEV. Reference [9] discussed all the electroweak phase transition patterns in the real singlet scalar extension to the SM. In this work, we discuss the above-mentioned scenario because we do not want to mix the Higgs field and the singlet scalar field at zero temperature. One reason for this choice is that the real singlet scalar S can be a good dark matter candidate because S need not have interacted with any of the SM particles except the Higgs boson. Even though we have not performed any analysis on dark matter physics in this paper, this model can be used as the starting point of our future works. On the other hand, at zero temperature, if there is no mixing between the Higgs field and the singlet scalar field, the Higgs portal coupling λ_m is completely a free parameter. Therefore, we can tune λ_m as much as possible to get enough strong first-order phase transitions, unlike the case where it depends on the Higgs singlet mixing angle $\sin\theta$, which is constrained by the LHC electroweak precision data when they mix. So, all bare parameters can be written in terms of physical, measurable quantities at zero temperature:

$$\mu_h^2 = \frac{m_h^2}{2}, \qquad \lambda_h = \frac{\mu_h^2}{v_{\rm EW}^2}, \quad \mu_s^2 = -m_S^2 + \frac{1}{2}\lambda_m v_{\rm EW}^2. \tag{5}$$

Therefore, the input parameters for this scenario are the mass of the Higgs boson, $m_h = 125$ GeV; the VEV of the Higgs field, $v_{\rm EW} = 246$ GeV; the mass and quartic coupling of the singlet scalar, m_S and λ_S, respectively; and the Higgs portal coupling, λ_m. Here, we consider the zero-temperature one-loop Coleman-Weinberg (CW) potential in the dimensional regularization schemes to avoid the infrared divergences which appear from the massless Goldstone modes at zero temperature in the on-shell renormalization schemes. For detailed calculations on infrared divergence, see Ref. [23]. We will talk about zero-temperature CW potential in both on-shell and as dimensional regularization schemes in a later section.

A. Field-dependent masses

In a general way, the 2×2 symmetric mass-squared matrix for the Higgs and singlet scalar in terms of a classical background field can be written as

$$M^2(h,S) = \begin{pmatrix} \frac{\partial^2 V}{\partial h^2} & \frac{\partial^2 V}{\partial h \partial S} \\ \frac{\partial^2 V}{\partial h \partial S} & \frac{\partial^2 V}{\partial S^2} \end{pmatrix} \equiv \begin{pmatrix} M_{hh}^2(h,S) & M_{hS}^2(h,S) \\ M_{hS}^2(h,S) & M_{SS}^2(h,S) \end{pmatrix}, \tag{6}$$

where

$$M_{hh}^2(h,S) = 3\lambda_h h^2 - \mu_h^2 + \frac{1}{2}\lambda_m S^2, \qquad M_{SS}^2(h,S) = \frac{1}{2}\lambda_m h^2 - \mu_S^2 + 3\lambda_S S^2, \qquad M_{hS}^2(h,S) = \lambda_m h S. \tag{7}$$

After diagonalization of the above mass-squared matrix, $M^2(h,S)$, the eigenvalues of the mass matrix give the field-dependent masses of the Higgs and singlet scalar:

$$\begin{aligned} m_{h_1}^2(h,S) &= \frac{1}{2}\left\{ m_{hh}^2(h,S) + m_{SS}^2(h,S) + \sqrt{(m_{hh}^2(h,S) - m_{SS}^2(h,S))^2 - 4m_{hS}^4(h,S)} \right\}, \\ m_{h_2}^2(h,S) &= \frac{1}{2}\left\{ m_{hh}^2(h,S) + m_{SS}^2(h,S) - \sqrt{(m_{hh}^2(h,S) - m_{SS}^2(h,S))^2 - 4m_{hS}^4(h,S)} \right\}. \end{aligned} \tag{8}$$

The field-dependent masses of other degrees of freedom are given by

$$\begin{aligned} m_W^2(h,S) &= \frac{g^2}{4}h^2, \qquad m_Z^2(h,S) = \frac{g'^2+g^2}{4}h^2, \qquad m_t^2(h,S) = \frac{1}{2}y_t^2 h^2, \\ m_{\chi_{1,2,3}}^2(h,S) &= -\mu_h^2 + \lambda_h h^2 + \frac{1}{2}\lambda_m S^2, \end{aligned} \tag{9}$$

where y_t is the Yukawa coupling for the top quark, and $\chi_{1,2,3}$ are the Goldstone bosons, as mentioned above. $m_W(h,S)$, $m_Z(h,S)$, and $m_t(h,S)$ are the field-dependent masses of the W boson, Z boson, and top quark, respectively.

From the perturbative unitarity condition, the coupling constants are constrained in the following ways:

$$\lambda_h < 4\pi, \qquad \lambda_S < 4\pi, \qquad |\lambda_m| < 8\pi, \qquad 3\lambda_h + 2\lambda_S + \sqrt{(3\lambda_h - 2\lambda_S)^2 + 2\lambda_m^2} < 8\pi. \tag{10}$$

For the potential to be bounded from below, the vacuum stability conditions should follow

$$\lambda_h > 0, \qquad \lambda_S > 0, \qquad \lambda_m > -2\sqrt{\lambda_h \lambda_S}. \tag{11}$$

Detailed calculations for perturbative unitarity can be found in Refs. [24,25], and for vacuum stability in Ref. [26].

III. ONE-LOOP EFFECTIVE POTENTIAL AT FINITE TEMPERATURE

The one-loop effective potential at nonzero temperature is given by [27]

$$V^T_{1-\text{loop}}(h,S,T) = \frac{T^4}{2\pi^2}\left[\sum_B n_B J_B\left(\frac{m_B^2(h,S)}{T^2}\right) + \sum_F n_F J_F\left(\frac{m_F^2(h,S)}{T^2}\right)\right]. \tag{12}$$

Here, B stands for all bosonic degrees of freedom that couple directly to the Higgs boson, therefore, $B = \{W, Z, h_1, h_2, \chi_{1,2,3}\}$, and F stands for only the top quark fermion. J_B and J_F are the thermal bosonic and fermionic functions which are given as follows:

$$J_B\left(\frac{m_B^2(h,S)}{T^2}\right) = \int_0^\infty dx x^2 \log\left(1 - e^{-\sqrt{x^2 + \frac{m_B^2(h,S)}{T^2}}}\right), \tag{13}$$

$$J_F\left(\frac{m_F^2(h,S)}{T^2}\right) = \int_0^\infty dx x^2 \log\left(1 + e^{-\sqrt{x^2 + \frac{m_F^2(h,S)}{T^2}}}\right). \tag{14}$$

We consider only the top quark contribution here since other fermionic contributions of the SM are less dominant because of small Yukawa coupling. If field-dependent masses at a given temperature are much less than the temperature of the plasma (i.e., $\frac{m_i^2}{T^2} \ll 1$), the thermal function admits a high-temperature expansion that will be very useful for practical applications. It is given by [27]

$$J_B\left[\frac{m_B^2}{T^2}\right] = -\frac{\pi^4}{45} + \frac{\pi^2}{12T^2} m_B^2 - \frac{\pi}{6T^3}(m_B^2)^{3/2} - \frac{1}{32T^4} m_B^4 \ln\frac{m_B^2}{a_b T^2} + \cdots, \tag{15}$$

$$J_F\left[\frac{m_F^2}{T^2}\right] = \frac{7\pi^4}{360} - \frac{\pi^2}{24T^2} m_F^2 - \frac{1}{32T^4} m_F^4 \ln\frac{m_F^2}{a_f T^2} + \cdots, \tag{16}$$

where $a_f = \pi^2 \exp(3/2 - 2\gamma_E)$ and $a_b = 16\pi^2 \exp(3/2 - 2\gamma_E)$, and the Euler constant, $\gamma_E = 0.577$. In Eq. (12), n_B and n_F represent the degrees of freedom of bosons and fermions:

$$n_W = 6, \qquad n_Z = 3, \qquad n_{h_1} = 1, \qquad n_{h_2} = 1, \qquad n_{\chi_{1,2,3}} = 1, \qquad n_t = -12. \tag{17}$$

For another limiting case, at a given temperature of plasma, if the field-dependent mass of a particle is much higher than the temperature (i.e., $\frac{m_i(h,S)^2}{T^2} \gg 1$), then the thermal functions, both bosonic and fermionic, behave like an exponentially decreasing function [28]. Therefore, in thermal effective potential, the contribution of a particle with a field-dependent mass greater than that of the temperature is almost negligible. The first terms on the right-hand sides of Eqs. (15) and (16) are independent of classical background fields; therefore, these terms are irrelevant in calculating the critical temperature, T_c.

In the dimensional regularization scheme, the temperature-independent Coleman-Weinberg (CW) potential term of the effective potential at one-loop order is given by [27]

$$V^{\text{CW}}_{1\text{-loop}}(h,S) = \frac{1}{64\pi^2}\left(\sum_B n_B m_B^4(h,S)\left[\log\left(\frac{m_B^2(h,S)}{Q^2}\right) - c_B\right] + \sum_F n_F m_F^4(h,S)\left[\log\left(\frac{m_F^2(h,S)}{Q^2}\right) - \frac{3}{2}\right]\right), \tag{18}$$

where B and F have been defined above, and $c_B = 3/2$ and $5/6$ for scalar and vector bosons, respectively. Q is the renormalization scale of the theory, which is taken to be $v_{\text{EW}} = 246$ GeV, the VEV of the Higgs field at zero temperature. Field-dependent masses of particles, $m_i(h,S) = \{m_B(h,S), m_F(h,S)\}$, are given in Eqs. (8) and (9), and all degrees of freedom, $n_i = \{n_B, n_F\}$, are given in Eq. (17).

A very useful scheme, called the cutoff regularization scheme, is obtained by regularizing the theory with a cutoff. Here, we add counterterms in the potential in such a way that the minima of the Higgs potential at $v_{\text{EW}} = 246$ GeV remain unchanged, and the Higgs and singlet scalar masses remain unchanged with respect to tree-level potential. So, the CW potential in the cutoff regularization scheme reads [27]

$$V^{\text{CW}}_{1\text{-loop}}(h,S) = \frac{1}{64\pi^2}\sum_{i=\{B\},\{F\}} n_i\left\{m_i^4(h,S)\left[\log\frac{m_i^2(h,S)}{m_i^2(v_{\text{EW}},0)} - \frac{3}{2}\right] + 2m_i^2(h,S)m_i^2(v_{\text{EW}},0)\right\}, \tag{19}$$

where $m_i^2(v_{\rm EW},0)$ is the square of the masses of particles in an electroweak vacuum (i.e., at $v_{\rm EW}=246$ GeV) with n_i degrees of freedom, and field-dependent mass-squared $m_i^2(h,S)$ formulas are given in Eq. (17) and in Eqs. (8), (9), respectively.

A. Thermal resummation

In order to reassure ourselves of the validity of the one-loop perturbative expansion, the corrections from the daisy resummation should be included in the one-loop potential. The leading-order resummation results give thermal corrections of $\Pi_i = d_i T^2$ to effective masses, where d_i values for different degrees of freedom in the plasma are given in Eq. (20). So, in our later numerical analysis, we have replaced bosonic masses: $m_i^2(h,S) \to m_i^2(h,S,T) = m_i^2(h,S) + d_i T^2$, where $d_i T^2$ is the finite-temperature contribution to the self-energies [29]:

$$\begin{aligned} d_{\chi_i} &= \frac{3}{16}g^2 + \frac{1}{16}g'^2 + \frac{1}{2}\lambda_h + \frac{1}{4}y_t^2 + \frac{1}{24}\lambda_m, \\ d_{hh} &= \frac{3}{16}g^2 + \frac{1}{16}g'^2 + \frac{1}{2}\lambda_h + \frac{1}{4}y_t^2 + \frac{1}{24}\lambda_m, \\ d_{SS} &= \frac{1}{4}\lambda_S + \frac{1}{6}\lambda_m, \qquad d_{Sh} \approx 0. \end{aligned} \tag{20}$$

Other than the self-energies correction to masses of Higgs bosons, singlet scalars, and Goldstone bosons, the thermal correction to masses of electroweak gauge bosons has been discussed in Refs. [30,31]. As the temperature correction to the masses of electrweak gauge bosons is very small compared to the field-dependent but temperature-independent mass terms, we do not consider the thermal correction of the electroweak gauge bosons in our numerical analysis. On the other hand, fermions cannot receive thermal correction to the masses because of gauge symmetry. A general and more rigorous treatment of the thermal resummation in calculating Π_i in the one-loop effective potential at finite temperature can be found in Ref. [32].

Here, we want to discuss the effective potential without the one-loop CW term and thermal resummation contributions at a very high temperature for analytic calculation purposes. At very high temperatures, where $m_i^2(h,S)/T^2 \ll 1$, we can take the high-temperature expansion of thermal functions that we have discussed before. But for better analysis of phase transition, we consider the full effective potential composing the tree-level term, the one-loop CW term, and the one-loop temperature-corrected term without taking any high-temperature approximation. Therefore, without considering the complicated CW term and daisy resummation contributions, in terms of the field-dependent part of the one-loop effective potential at very high temperature, we have

$$\begin{aligned} V(h,S,T) &= V_0(h,S) + V^T_{\text{1-loop}}(h,S,T) \\ &\approx -\frac{1}{2}\mu_h^2(T)h^2 + \frac{1}{4}\lambda_h h^4 - E^{\rm SM}Th^3 - \frac{1}{2}\mu_S^2(T)S^2 \\ &\quad + \frac{1}{4}\lambda_S S^4 + \frac{1}{4}\lambda_m h^2 S^2 - E(h,S)T, \end{aligned} \tag{21}$$

where the mass-squared parameters are defined by

$$\mu_h^2(T) = \mu_h^2 - c_h T^2, \qquad \mu_S^2(T) = \mu_S^2 - c_S T^2, \tag{22}$$

with μ_h^2 and μ_S^2 having the squared mass defined at $T=0$. All coefficients in the above Eqs. (21) and (22) are given by

$$\begin{aligned} c_h &= \frac{1}{48}[9g^2 + 3g'^2 + 2(6y_t^2 + 12\lambda_h + \lambda_m)], \\ E^{\rm SM} &= \frac{1}{32\pi}[2g^3 + \sqrt{g^2+g'^2}^3], \\ c_S &= \frac{1}{12}(2\lambda_m + 3\lambda_S), \\ E(h,S) &= \frac{1}{12\pi}[(m_{h_1}^2(h,S))^{3/2} + (m_{h_2}^2(h,S))^{3/2} \\ &\quad + 3(m_{\chi_1}^2(h,S))^{3/2}], \end{aligned} \tag{23}$$

where $m_{h_{1,2}}^2(h,S)$ and $m_{\chi_1}^2(h,S)$ are given in Eqs. (8) and (9).

IV. NUMERICAL ANALYSIS

The total effective potential can be written as

$$V_{\rm eff}^{\rm tot}(h,S,T) = V_0(h,S) + V^{\rm CW}_{\text{1-loop}}(h,S,T) + V^T_{\text{1-loop}}(h,S,T). \tag{24}$$

It needs to be mentioned that $V^{\rm CW}_{\text{1-loop}}(h,S,T)$ depends on the temperature explicitly due to the thermal resummation of masses from the daisy diagrams to maintain the validity of the perturbative expansion at one-loop level. Effectively, all three terms on the right-hand side of Eq. (24) also depend on the temperature implicitly through the VEV of Higgs, v, and the singlet scalar, w.

Here, we are interested in studying the first-order EWPT in that scenario where the phase transition occurs through a three-step process. At very high temperatures, both the Higgs and the singlet scalar fields have no VEV—i.e., the Universe was in a fully symmetric phase. When the temperature gradually decreases, the singlet scalar field S gets a VEV, w, but the Higgs field does not get a VEV—i.e., Z_2 symmetry breaks spontaneously, but electroweak symmetry is there. When temperature further decreases, the Higgs field gets a VEV, v, but the singlet scalar has no VEV—i.e., electroweak symmetry breaks spontaneously, but Z_2 symmetry is restored. For a given parameter space, the conditions for calculating the critical temperature, T_c, and the VEV of the Higgs field, v_c, at T_c are given by

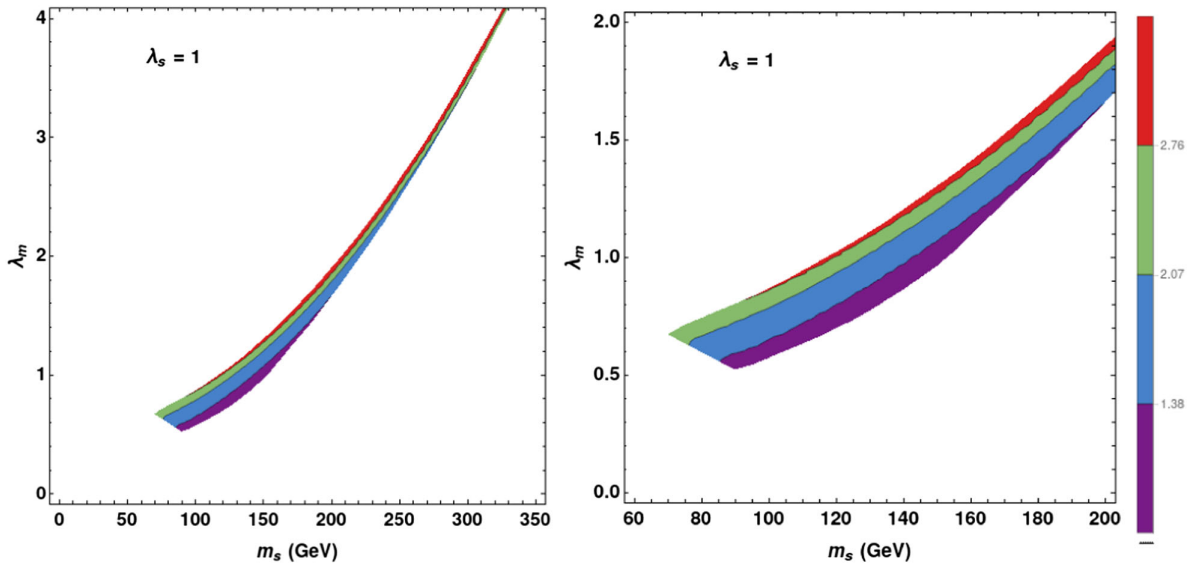

FIG. 1. Allowed region in the $\lambda_m - m_S$ (GeV) plane for $\lambda_S = 1$, where different colors represent the phase transition strength. The right panel shows a zoomed-in version of the left panel up to $\lambda_m = 2$.

$$V_{\text{eff}}^{\text{tot}}(v_c, 0, T_c) = V_{\text{eff}}^{\text{tot}}(0, w_c, T_c) \tag{25}$$

$$\left.\frac{dV_{\text{eff}}^{\text{tot}}(h, S, T_c)}{dh}\right|_{h=v_c, S=0, T_c} = 0,$$

$$\left.\frac{dV_{\text{eff}}^{\text{tot}}(h, S, T_c)}{ds}\right|_{h=0, S=w_c, T_c} = 0. \tag{26}$$

Here, v_c and w_c are the VEVs of the Higgs field and singlet scalar field, respectively, at the critical temperature. Analytically, it is impossible to solve the above three Eqs. (25) and (26) simultaneously. So, we perform a scan over the parameter space, numerically imposing the following condition for first-order EWPT. The necessary condition for first-order EWPT is that

$$\frac{v_c}{T_c} \geq 1. \tag{27}$$

In order to calculate T_c and v_c from Eqs. (25) and (26), we cannot get the exact solution of the three above-mentioned equations. Therefore, for numerical scanning, we solve Eq. (25) within 1% error.

In Figs. 1 and 2, we have shown the allowed region in λ_m and m_S parameter space for a fixed λ_S provided first-order EWPT. The different colors of the figures represent the strength, $\frac{v_c}{T_c}$, of the phase transition. In other words, the higher the value of $\frac{v_c}{T_c}$, the stronger the phase transition. In the left panel of Fig. 1, we have shown the variation of λ_m with respect to m_S for $\lambda_S = 1$ for first-order EWPT. From this figure we can see that first-order EWPT can be achieved for higher values of m_S only when the value of λ_m is increased. For $m_S \leq 70$ GeV, which corresponds to $\lambda_S = 1$, we cannot observe any signature for strong first-order EWPT. We can clearly understand from this figure that after a certain value of m_S, the parameter space gets constrained. The right panel of Fig. 1 shows a zoomed-in version of the left panel, where a wider range in the parameter space can be found up to $\lambda_m = 2$; the region almost corresponds to the electroweak scale. In this electroweak region, we get a wider parameter space in the $\lambda_m - m_S$ plane, because if $m_S \gg$ electroweak scale, then the scalar decouples from the SM Higgs. For this mass region of m_S, the contribution of the singlet scalar becomes negligible in the effective potential.

In the left panel of Fig. 2, we have shown the allowed parameter space in the $\lambda_m - m_S$ plane for $\lambda_S = 0.5$. From this figure, we can see that we cannot get any parameter space for $m_S \leq 65$ GeV. The right panel of this figure shows the variation of λ_m with respect to m_S for $\lambda_S = 0.1$. From this figure, we see that we cannot get a wider parameter space for higher values of m_S with compare to $\lambda_S = 1$ and $\lambda_S = 0.5$ scenarios. This is because for such low values of λ_S, the potential is not bounded from below for higher values of m_S, and we cannot get any stable minima (w) for S. By comparing all the figures, we can see an allowed parameter space in the $\lambda_m - m_S$ plane for lower values of m_S and λ_m when λ_S is also lower. Here, we have considered the $\overline{\text{MS}}$ renormalization scheme where the one-loop potential explicitly depends on the choice of renormalization scale Q. In order to reduce the scale dependence, an RGE improvement should be implemented on the one-loop CW potential [33,34]. We leave this implementation for future studies.

A. Calculation of entropy release into the plasma

In order to calculate the entropy release due to EWPT, one needs to take into account the energy and pressure

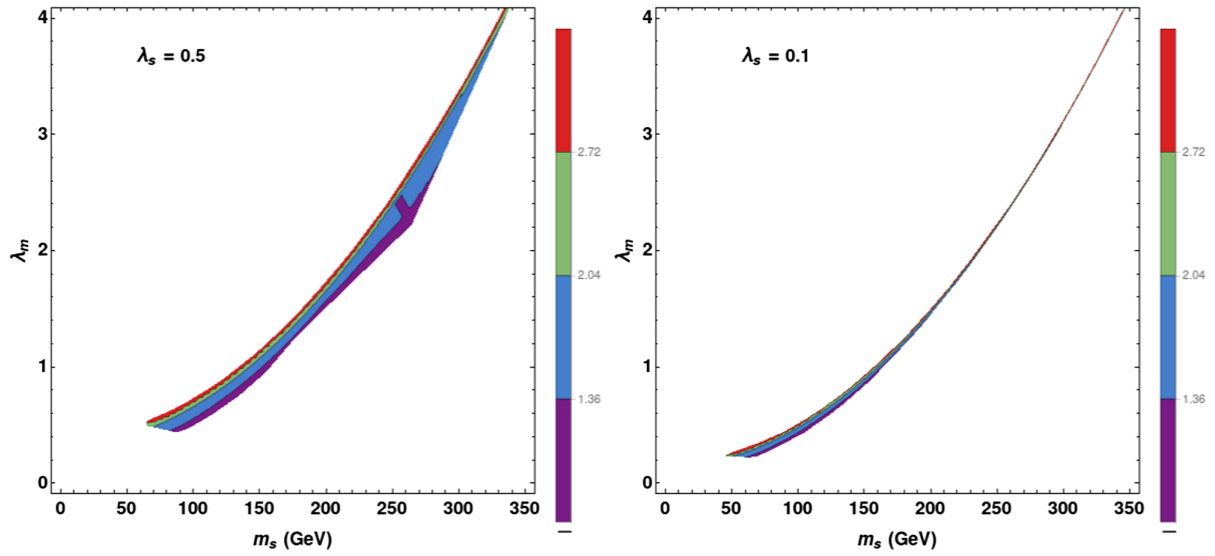

FIG. 2. Allowed region in the $\lambda_m - m_S$ (GeV) plane for $\lambda_S = 0.5$ (left panel) and $\lambda_S = 0.1$ (right panel) provided first-order EWPT. Here, different colors represent the phase transition strength, v_c/T_c.

density of the plasma at the instant of the phase transition. The energy and the pressure density can be calculated using the energy-momentum tensor ($T_{\mu\nu}$), which is given as

$$T_{\mu\nu} = \partial_\mu\phi\partial_\nu\phi + \partial_\mu S\partial_\nu S - g_{\alpha\beta}(g^{\alpha\beta}(\partial_\alpha\phi\partial_\beta\phi + \partial_\alpha S\partial_\beta S) - V^{\rm tot}_{\rm eff}(h,S,T)) + \text{SM fermions}. \quad (28)$$

The last part of Eq. (28) can be found in Ref. [6]. The fermionic sector remains the same as that of the SM, since the singlet scalar S does not modify the fermonic part.

During that epoch, the Universe can be assumed to be homogeneous and isotropic, and hence the spatial derivatives of the scalar and the Higgs field can be neglected. We further assume that the scalar and the Higgs field oscillate around their minima and that the damping rate of the oscillation is very high. Under these assumptions, the energy and the pressure density of the plasma are given by

$$\rho = \dot{\phi}^2_{\rm min} + \dot{S}^2_{\rm min} + V^{\rm tot}_{\rm eff}(h,S,T) + \frac{g_*\pi^2}{30}T^4, \quad (29)$$

$$\mathcal{P} = \dot{\phi}^2_{\rm min} + \dot{S}^2_{\rm min} - V^{\rm tot}_{\rm eff}(h,S,T) + \frac{1}{3}\frac{g_*\pi^2}{30}T^4. \quad (30)$$

The last terms in Eqs. (29) and (30) arise from the Yukawa interaction between fermions and Higgs bosons, and from the energy density of the fermions, the gauge bosons, and the interaction between the Higgs and gauge bosons. g_* depends on the effective number of particles present in the relativistic soup at or near the EWPT. Its value in our model is greater than the value in the SM.

As mentioned before in Eq. (1), the entropy density is conserved for relativistic species with negligible chemical potential. From Eqs. (29) and (30), we get

$$\rho + \mathcal{P} = 2\dot{\phi}^2_{\rm min} + 2\dot{S}^2_{\rm min} + \frac{4}{3}\frac{g_*\pi^2}{30}T^4. \quad (31)$$

It is evident that g_* will change with the decoupling process, and thus s for relativistic plasma will increase for our considered scenario. Then, the increase in entropy can be calculated using conservation law:

$$\dot{\rho} = -3H(\rho + \mathcal{P}). \quad (32)$$

Using the above assumptions, Eq. (32) takes the approximate form

$$\frac{\dot{T}}{T}\left[g_* v_c^2 T^2\left(1 - \frac{T^2}{T_c^2}\frac{g_*(m)}{g_*}\right) + \frac{4\pi^2 g_*}{30}T^4\right] = -\frac{4H\pi^2 g_*}{30}T^4, \quad (33)$$

where T is the temperature of the plasma, which is decreasing after the phase transition, v_c is the effective value of the potential at the moment of phase transition, $g_* \approx 107.75$ is the effective number of degrees of freedom of the whole system, $g_*(m)$ is the reduced number of effective degrees of freedom when certain species become nonrelativistic, and H is the Hubble parameter.

Due to the presence of the new scalar S, an analytical solution of Eq. (32) is not possible, and we revert to a numerical solution of the differential equation. We do not take into account the modification of the evolution due to the annihilation of nonrelativistic species—for example, the annihilation of e^+e^-, which takes place below the mass of the electron. This is disregarded, because if the annihilating particles are in a thermal equilibrium state with vanishing chemical potential, the entropy density in this process is conserved.

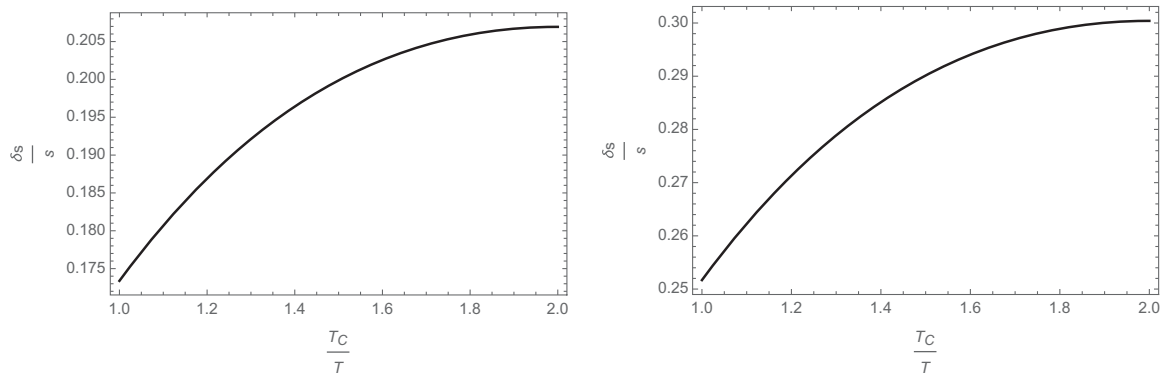

FIG. 3. The relative increase in entropy for the two BM points. **BM1**: $v_c = 150.56$ GeV, $T_c = 116$ GeV, $v_c/T_c = 1.298$, $m_S = 120$ GeV, $\lambda_m = 0.77$, $\lambda_S = 1$, and $\delta s/s \sim 20\%$. **BM2**: $v_c = 202.41$ GeV, $T_c = 82$ GeV, $v_c/T_c = 2.47$, $m_S = 160$ GeV, $\lambda_m = 1.35$, $\lambda_S = 1$, and $\delta s/s \sim 30\%$. As can be seen from the graph, the amount of entropy influx into the plasma is dependent on the strength of the phase transition. Clearly, for the BM with a higher value of v_c/T_c, a higher entropy influx into the plasma is observed.

For $T \gg T_c$, the Universe is in thermal equilibrium, and relativistic particles dominate the Universe. The contribution to the overall energy density of the Universe from those that are already massive (e.g., decoupled DM) is also insignificant. To this extent, the entropy density per unit comoving volume follows the conservation law, as mentioned in Eq. (1). In this scenario, the sum of the energy and the pressure density can lead up to

$$\rho_r + \mathcal{P}_r \sim g_* T^4. \tag{34}$$

It is to be noted that g_* is not constant, but it varies over time. It depends on the components of the primordial plasma. And hence,

$$T \sim a^{-1}. \tag{35}$$

It is worthwhile to mention that the conserved quantity is $s = g_*(T)a^3T^3$. But while estimating the amount of entropy released, we calculated a^3T^3. This is because the contribution to entropy is dominated by the heaviest particle in the temperature range $m(h, S, T) < T$. So for these temperatures, $g_*(T)T = \text{const.}$, and the relative entropy rise is given just by a^3T^3. Since the final temperature $T_f = m(h, S, T_f)$, below which new particle species start to dominate, is not dependent upon g_*, the relative increase of entropy is determined by T^3a^3. Thus, the rise in entropy is dominated by the change in the scale factor (i.e., a^3T^3), suggesting the influx of entropy happening over $g_*a^3T^3$. And hence, the net entropy release is given by the generic expression

$$\frac{\delta s}{s} = \frac{(a_c T_c)^3 - (aT)^3}{(a_c T_c)^3}, \tag{36}$$

where a_c and T_c are the cosmological scale factor and the temperature of the plasma when the phase transition took place.

Following the above assumptions, for two sets of benchmark (BM) points, the relative rise in entropy is shown in Fig. 3.

V. IMPACT ON STOCHASTIC GRAVITATIONAL WAVES

First-order phase transition in the early Universe can be a source of stochastic gravitational waves (GWs). In general, the phase transition took place around $\sim 10^{-11}$ sec after the big bang, well before the onset of big bang nucleosynthesis. As the temperature of the Universe cools down, it starts undergoing a first-order phase transition which takes place at $T = T_c$. Above this temperature, the symmetry of the Universe is restored. But as the temperature falls below T_c, a second degenerate minima appears, denoting first-order phase transition. After the phase transition, the latent heat is released, and a small portion of it goes to the GW; the rest goes back to the plasma.

The GW, which is generated due to the FOPT, depends on two parameters—namely, α and β, which denote the strength of the phase transition and the inverse time during the phase transition, respectively. More details on these parameters can be found in Refs. [35,36], etc. The parameter α is defined as

$$\alpha = \frac{\epsilon}{\rho_{\text{rad}}}, \tag{37}$$

where $\rho_{\text{rad}} = \frac{\pi^2 g_*}{30} T^4$ is the energy density of radiation, and ϵ is the potential energy of the scalar field that includes the latent energy density and is given by

$$\epsilon = \left(V - T\frac{\partial V}{\partial T}\right)\Big|_{(\phi_{\text{high}}, T_*)} - \left(V - T\frac{\partial V}{\partial T}\right)\Big|_{(\phi_{\text{low}}, T_*)}, \tag{38}$$

where the subscript $*$ denotes the time at which the phase transition took place [37], and high (low) denotes the field

value at high (low) vacuum. In this work, we take $T_* = T_c$. For brevity, β is normalized as $\tilde{\beta} = \beta/H(T = T_c)$, where $H(T = T_c)$ is the value of the Hubble rate at $T = T_c$. It is expressed as

$$\tilde{\beta} = \left[T\frac{dS_{\rm E}(T)}{dt}\right]\Big|_{T=T_c}, \tag{39}$$

where $S_{\rm E}(T)$ is the three-dimensional Euclidean action and is given by

$$S_{\rm E}(T) = \int d^3x \left[\frac{1}{2}(\partial_\mu \phi)^2 + V_{\rm eff}(\phi, T)\right]. \tag{40}$$

Here, $V_{\rm eff}(\phi, T)$ is the effective potential and can be generalized to take the form of Eq. (24). For more details, see Ref. [38].

The energy density of the GW has three components,

$$\Omega_{\rm GW}h^2 = \Omega_\phi h^2 + \Omega_{\rm SW}h^2 + \Omega_{\rm turb}h^2. \tag{41}$$

In the above Eq. (41), h is the dimensionless Hubble rate, Ω_ϕ is the scalar field contribution (here the contribution comes from the singlet scalar S as introduced before), $\Omega_{\rm SW}$ is the sound wave contribution which surrounds the bubble wall, and $\Omega_{\rm turb}$ is the contribution which comes from the magnetohydrodynamic turbulence in the plasma. Detailed discussion and numerical simulations regarding these three parameters can be found in Refs. [39–52].

In what follows, we are interested in the dilution of this energy density as a result of the entropy release during the first-order electroweak phase transition. This entropy suppression factor $\mathcal{S} = \frac{\delta s}{s}$ has little to no effect to the second and third terms in Eq. (41), as they are not related to the BSM particles and field. They simply appear due to the phase transition and bubble nucleation. Moreover, $\Omega_{\rm SW}h^2$ is suppressed heavily due to the finite lifetime of the sound waves—see Ref. [53].

For our scenario where the phase transition takes place in such a way that neither the singlet nor the Higgs has a nonzero VEV at the same moment, the third term also does not play much role in contributing to the energy density of the GW. It is not negligible, but for brevity, we consider that the primary contribution to the GW comes from the first term, which in turn gets diluted during the process of strong first-order electroweak phase transition (SFOEWPT) due to the release of the entropy. And hence, during this process, the diluted energy density $\Omega_{\rm GW}h^2|_{\rm dil}$ is approximated as

$$\Omega_{\rm GW}h^2|_{\rm dil} = \mathcal{S}\Omega_{\rm GW}h^2. \tag{42}$$

And from Eq. (42), the dilution factor can be otherwise written as

$$\frac{\delta(\Omega_{\rm GW}h^2)}{\Omega_{\rm GW}h^2} = \frac{\Omega_{\rm GW}h^2|_{T>T_c} - \mathcal{S}\Omega_{\rm GW}h^2|_{T<T_c}}{\Omega_{\rm GW}h^2|_{T>T_c}}. \tag{43}$$

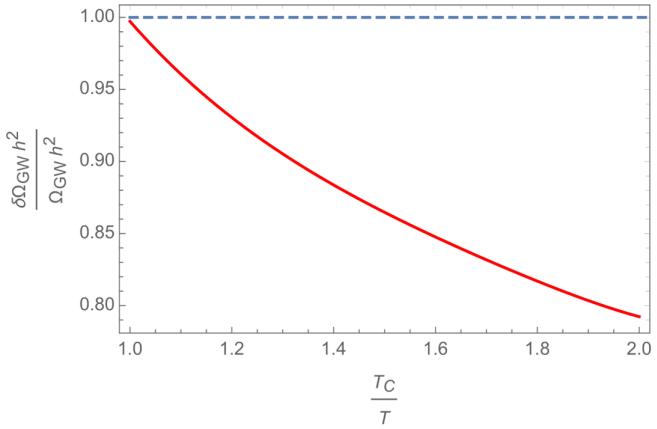

FIG. 4. The red line shows the dilution of the energy density of the gravitational waves during the SFOEWPT. The dotted line shows the hypothetical scenario where entropy release did not take place and the suppression/dilution of the energy density of the GW did not happen.

Evidently, before the onset of the phase transition, when the net entropy release is $\frac{\delta s}{s} = 0$, the second term on the numerator of the rhs is 0, and the lhs is equal to 1. This can be clearly seen from Fig. 4. Figure 4 is made while keeping in mind that the parameter space of the phase transition follows BM1, where the mass of the scalar is 120 GeV and the transition takes place at 116 GeV.

It is clear from Fig. 4 that during the process of the strong first-order phase transition, as entropy influx into the plasma takes place, the energy density of the gravitational waves is diluted. This dilution depends strongly on the parameter space of the phase transition. For stronger first-order phase transition, for example, with multiple Higgs fields, the dilution can be severe as compared to the scenario shown here.

There can be other effects of the this dilution—for example, dilution of the frozen out dark matter species [22] and baryon asymmetry. This can also lead to electroweak baryogenesis and baryo-through-leptogenesis as well.

VI. CONCLUSION

It is shown in this paper that with the inclusion of a real singlet scalar S to the SM and imposing an extra Z_2 symmetry, the EWPT becomes a first-order phase transition. Possible benchmark points which can lead to this first-order phase transition are studied and discussed in detail. In the latter part of the paper, the entropy release due to this first-order EWPT is studied for two benchmark points numerically, which are shown in Fig. 3. This is followed by connecting this release of entropy into the plasma with the dilution of stochastic GWs. It can be seen from Fig. 4 that the net dilution factor of the GWs is almost the same as that of the release of entropy.

The stronger the phase transition is, the higher the amount of entropy produced. The production can be even

larger when a singlet scalar extension to the two-Higgs-doublet model is considered. But this is beyond the scope of this paper and will be studied in subsequent papers.

ACKNOWLEDGMENTS

The authors expresses their thanks to Kousik Loho and Professor Baradhwaj Coleppa for useful discussion. The work of A. C. is partly funded by an APEX project offered by IOP-B and partly by a SERB project titled "Higgs physics beyond the Standard Model at the LHC" (RES/SERB/PH/P0202/2021/0039). J. D. acknowledges the Council of Scientific and Industrial Research (CSIR), government of India, for a SRF fellowship grant with File No. 09/045(1511)/2017-EMR-I. J. D. also acknowledges research Grant No. CRG/2018/004889 of the SERB, India.

[1] Sean M. Carroll, Zachary H. Rhoades, and Jon Leven, *Dark Matter, Dark Energy: The Dark Side of the Universe. Guidebook Part 2* (The Teaching Company, Chantilly, VA, 2007), p. 59.
[2] A. D. Sakharov, Pis'ma Zh. Eksp. Teor. Fiz. **5**, 32 1967.
[3] P. A. R. Ade *et al.* (Planck Collaboration), Astron. Astrophys. **594**, A13 (2016).
[4] E. W. Kolb and M. S. Turner, Front. Phys. **69**, 1 (1990).
[5] CMS Collaboration, Phys. Lett. B **716**, 30 (2012).
[6] A. Chaudhuri and A. Dolgov, J. Cosmol. Astropart. Phys. 01 (2018) 032.
[7] K. Kajantie, M. Laine, K. Rummukainen, and M. Shaposhnikov, Phys. Rev. Lett. **77**, 2887 (1996).
[8] D. E. Morrissey and M. J. Ramsey-Musolf, New J. Phys. **14**, 125003 (2012).
[9] M. Carena, Z. Liu, and Y. Wang, J. High Energy Phys. 08 (2020) 107.
[10] C. W. Chiang and B. Q. Lu, J. High Energy Phys. 07 (2020) 082.
[11] Z. Kang, P. Ko, and T. Matsui, J. High Energy Phys. 02 (2018) 115.
[12] A. Chaudhuri and M. Yu. Khlopov, Universe **7**, 275 (2021).
[13] B. Abi *et al.* (Muon $g-2$ Collaboration), Phys. Rev. Lett. **126**, 141801 (2021).
[14] T. Boeckel, S. Schettler, and J. S. Bielich, Prog. Part. Nucl. Phys. **66**, 266 (2011).
[15] A. Chaudhuri and A. Dolgov, J. Exp. Theor. Phys. **133**, 552 (2021).
[16] A. D. Dolgov, P. D. Naselsky, and I. D. Novikov, arXiv: astro-ph/0009407.
[17] S. Blashi and A. Mariotti, arXiv:2203.16450.
[18] P. Huet and A. E. Nelson, Phys. Rev. D **53**, 4578 (1996).
[19] A. I. Bochkarev, S. V. Kuzmin, and M. E. Shaposhnikov, Phys. Lett. B **244**, 275 (1990).
[20] A. Chaudhuri and M. Yu. Khlopov, Physics **3**, 275 (2021).
[21] A. Chaudhuri, M. Yu. Khlopov, and S. Porey, Galaxies **9**, 45 (2021).
[22] A. Chaudhuri, M. Yu. Khlopov, and S. Porey, Symmetry **14**, 271 (2022).
[23] J. Elias-Miro, J. R. Espinosa, and T. Konstandin, J. High Energy Phys. 08 (2014) 034.
[24] R. Zhou, J. Yang, and L. Bian, J. High Energy Phys. 04 (2020) 071.
[25] K. Kannike, K. Loos, and M. Raidal, Phys. Rev. D **101**, 035001 (2020).
[26] K. Kannike, Eur. Phys. J. C **76**, 324 (2016); **78**, 355(E) (2018).
[27] M. Quiros, Helv. Phys. Acta **67**, 451 (1994).
[28] C. Delaunay, C. Grojean, and J. D. Wells, J. High Energy Phys. 04 (2008) 029.
[29] M. E. Carrington, Phys. Rev. D **45**, 2933 (1992).
[30] K. Hashino, M. Kakizaki, S. Kanemura, and T. Matsui, Phys. Rev. D **94**, 015005 (2016).
[31] P. Bandyopadhyay and S. Jangid, arXiv:2111.03866.
[32] D. Curtin, P. Meade, and H. Ramani, Eur. Phys. J. C **78**, 787 (2018).
[33] A. Andreassen, W. Frost, and M. D. Schwartz, Phys. Rev. D **91**, 016009 (2015).
[34] A. Andreassen, W. Frost, and M. D. Schwartz, Phys. Rev. Lett. **113**, 241801 (2014).
[35] H. Shibuya and T. Toma, arXiv:2207.14662v1.
[36] N. Okada and O. Seto, Phys. Rev. D **98**, 063532 (2018).
[37] P. Binetruy, A. Bohe, C. Caprini, and J. F. Dufaux, J. Cosmol. Astropart. Phys. 06 (2012) 027.
[38] B. Fornal and E. Pierre, arXiv:2209.04788v1.
[39] A. Kosowsky, M. S. Turner, and R. Watkins, Phys. Rev. D **45**, 4514 (1992).
[40] A. Kosowsky, M. S. Turner, and R. Watkins, Phys. Rev. Lett. **69**, 2026 (1992).
[41] A. Kosowsky and M. S. Turner, Phys. Rev. D **47**, 4372 (1993).
[42] M. Kamionkowski, A. Kosowsky, and M. S. Turner, Phys. Rev. D **49**, 2837 (1994).
[43] C. Caprini, R. Durrer, and G. Servant, Phys. Rev. D **77**, 124015 (2008).
[44] S. J. Huber and T. Konstandin, J. Cosmol. Astropart. Phys. 09 (2008) 022.
[45] M. Hindmarsh, S. J. Huber, K. Rummukainen, and D. J. Weir, Phys. Rev. Lett. **112**, 041301 (2014).
[46] M. Hindmarsh, S. J. Huber, K. Rummukainen, and D. J. Weir, Phys. Rev. D **92**, 123009 (2015).
[47] C. Caprini and R. Durrer, Phys. Rev. D **74**, 063521 (2006).
[48] T. Kahniashvili, A. Kosowsky, G. Gogoberidze, and Y. Maravin, Phys. Rev. D **78**, 043003 (2008).
[49] T. Kahniashvili, L. Campanelli, G. Gogoberidze, Y. Maravin, and B. Ratra, Phys. Rev. D **78**, 123006 (2008); **79**, 109901(E) (2009).

[50] T. Kahniashvili, L. Kisslinger, and T. Stevens, Phys. Rev. D **81**, 023004 (2010).
[51] C. Caprini, R. Durrer, and G. Servant, J. Cosmol. Astropart. Phys. 12 (2009) 024.
[52] P. Binetruy, A. Bohe, C. Caprini, and J. F. Dufaux, J. Cosmol. Astropart. Phys. 06 (2012) 027.
[53] H. K. Guo, K. Sinha, D. Vagie, and G. White, J. Cosmol. Astropart. Phys. 01 (2021) 001.